

**Dieses Dokument ist eine Zweitveröffentlichung (Verlagsversion) /  
This is a self-archiving document (published version):**

Andreas Voigt, Uwe Marschner, Andreas Richter

## **Multiphysics equivalent circuit of a thermally controlled hydrogel microvalve**

**Erstveröffentlichung in / First published in:**

*Journal of Intelligent Material Systems and Structures*. 2017, 28(16), S. 2265 - 2274 [Zugriff am: 12.08.2019]. SAGE journals. ISSN 1530-8138.

DOI: <https://doi.org/10.1177/1045389X16685445>

Diese Version ist verfügbar / This version is available on:

<https://nbn-resolving.org/urn:nbn:de:bsz:14-qucosa2-356280>


„Dieser Beitrag ist mit Zustimmung des Rechteinhabers aufgrund einer (DFGgeförderten) Allianz- bzw. Nationallizenz frei zugänglich.“

This publication is openly accessible with the permission of the copyright owner. The permission is granted within a nationwide license, supported by the German Research Foundation (abbr. in German DFG).

[www.nationallizenzen.de/](http://www.nationallizenzen.de/)

# Multiphysics equivalent circuit of a thermally controlled hydrogel microvalve

Andreas Voigt, Uwe Marschner and Andreas Richter

*Journal of Intelligent Material Systems and Structures*  
2017, Vol. 28(16) 2265–2274  
© The Author(s) 2017  
Reprints and permissions:  
sagepub.co.uk/journalsPermissions.nav  
DOI: 10.1177/1045389X16685445  
journals.sagepub.com/home/jim  


## Abstract

Temperature-responsive hydrogels are polymer particles whose equilibrium size depends on the temperature of the water they are immersed in. Here we present an equivalent circuit model of a temperature-controlled microvalve based on hydrogel particles. The resulting network model consists of three physical subsystems. The thermal subsystem considers the heat capacities and thermal resistances of the layers of the valve and the coupling to the ambient environment. The polymeric subsystem describes the relaxation of the hydrogel particles to the temperature-dependent equilibrium size. The fluidic subsystem consists of the supply channel and a chamber whose cross section varies according to the size of the hydrogel particles. All subsystems are described and coupled within one single circuit. Thus the transient behavior of the valve can be calculated using a circuit simulator. Simulation results for a setup are presented and compared with experiments.

## Keywords

Circuit representation, equivalent circuit, microvalve, multiphysics modeling, network modeling, stimuli-responsive hydrogels, stimuli-sensitive hydrogels, thermal control

## Introduction

Hydrogels consist of a network of crosslinked polymers that swell when put into water. The equilibrium size of a stimuli-sensitive hydrogel depends on a thermodynamic or chemical property of the aqueous solution in which it is placed. There are hydrogels which are sensitive to temperature, pH-value or the concentration of chemicals in the solution. By placing these hydrogels in a chamber, valves can be built that are controlled by means other than pneumatic actuation (Arndt et al., 2000). A particularly promising application is the construction of hydrogel-based microvalves for flow control in labs-on-chips. In Beebe et al. (2000) a pH-sensitive hydrogel was proposed for flow sorting. Baldi et al. (2003) constructed a hydrogel-valve which employs the concentration of glucose as a trigger. In Ehrenhofer et al. (2016) a hydrogel-valve in a switchable pore set-up was presented. In Paschew et al. (2016) a hydrogel-valve triggered by the concentration of 1-Propanol was used to build an autonomous chemofluidic oscillator circuit, demonstrating the feasibility of these smart valves for inherent feedback. The temperature-controlled hydrogel-based microvalve described by Richter et al. (2003, 2004a,b) has the advantages of simple setup, small dead volume, good

particle tolerance, good sealing, easy miniaturization and integrability into microsystems.

Here we present a dynamic multi-physics model and simulation of this temperature-controlled valve and compare it with experimental measurements. The model can be used to calculate the dynamic response of the flow rate through the valve to the application of an arbitrary time-dependent heating power. It gives insight and an understanding of the relevant (chemo-)physical processes. Based on the material and geometrical parameters of the design, it can be used for an optimization of the valve. Further it can be employed to access quantities that are difficult to obtain by experiment. In addition, it can be easily integrated into systems of more than one valve.

We utilize a network representation, that is, an equivalent circuit (Lenk et al., 2011)), for the modeling of the valve. The network represents a system of

---

Institute of Semiconductors and Microsystems, Technische Universität Dresden, Germany

### Corresponding author:

Andreas Voigt, Chair of Polymeric Microsystems, Institute of Semiconductors and Microsystems, Technische Universität Dresden, 01062 Dresden, Germany.  
Email: andreas.voigt@tu-dresden.de

coupled ordinary differential equations with variables grouped as difference coordinates or flow coordinates. It is a lumped model (also known as compact model) in the sense that an “infinite-dimensional” system characterized by (electric, magnetic, mechanical, acoustic, chemical, etc.) fields, whose evolution is determined by partial differential equations, is approximated by a small number of degrees of freedom and material and geometrical parameters. The gain is an often increased degree of intuitive handling and a faster simulation, at the cost of a potential decrease of accuracy or discretization artifacts. An important condition for the discretization process is, that the wavelengths of propagating signals must be at least four times as large as the largest dimension of the discretized elements. Equivalent circuits are abundant in the semiconductor industry for modeling and simulating electronic devices (Pierret and Sah, 1970a,b; Sah, 1970). It is also interesting to note that the well-known Hodgkin–Huxley model of signal transduction in neurons is a network model (Hodgkin and Huxley, 1952). Besides the application in electronics, circuits can also be applied to describe mechanical (Marschner et al., 2009), acoustic, fluidic or thermal processes. Typical elements of these circuits describe inertia, dissipation, storage and sources of the difference or flow coordinate. Their differential equations are isomorphic to those of inductors, resistors, capacitors, voltage sources and current sources in electronics, respectively. A particular strength of a network representation is the description of multi-physics systems in one single circuit (Marschner et al., 2013), where the coupling of the domains is achieved via transducers. Compared to a textual representation by equations the network description has the advantage of a structural representation that is intuitive and easy to analyze, modify and augment. The system can be simulated efficiently by current circuit simulators. LTspice uses the SPICE kernel, a solver for ordinary differential equations that has been highly optimized in its more than 40 years of existence. In addition, the distribution of one single simulation task to several processor cores is supported (Brocard and Engelhardt, 2011). The fast simulation time and the interface provided also facilitate parameter studies for design optimization or robustness studies for parameter variations with random distributions (e.g. due to the fabrication process). One trend on the way towards microfluidic design automation is the utilization of the electronic–hydraulic analogy for microfluidic circuit design (Li and Cheng, 2013; Oh et al., 2012; Perdigones et al., 2014). Here, network models of components potentially play a big role, as they are easy to integrate into the context of microfluidic circuits.

We first outline the setup of the hydrogel-based microvalve. Then we successively describe the modeling of the thermal, polymeric and fluidic domains. Then implementation details for the simulation of the system

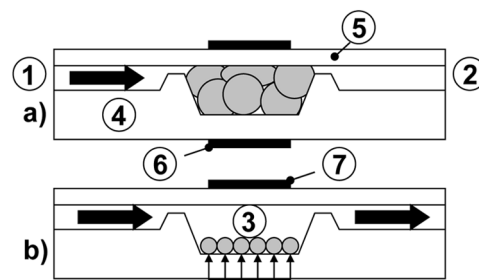


**Figure 1.** Schematic of the microvalve: (1) inlet, (2) outlet, (3) actuator chamber filled with hydrogel particles, (4) structure layer, (5) Pyrex cover layer, (6) heater (located at back side), (7) temperature sensor (located at top side); (a) closed state, (b) open state.

with LTspice are discussed. The results of the simulation are compared with the experimentally measured behavior of the microvalve. We end the article with a conclusions section and an outlook of future work.

## Microvalve construction

The microvalve (Figure 1) acts as a fluidic resistor whose resistance depends on the degree of swelling of the hydrogel particles employed. The hydrogel particles are placed in a chamber (3) formed by a structured Silicon layer (4) and a flat Pyrex cover plate (5). The hydrogels are fabricated from Poly(N-isopropylacrylamide), crosslinked by N,N-methylene-bisacrylamide. The temperature of the water in the chamber and the particles contained can be changed by a thin-film resistive heater (6) attached to the bottom of the Silicon layer. The temperature at the top of the Pyrex plate is measured via a thin-film resistive platinum sensor (7). Water is guided to the chamber via an inlet (1) and an outlet (2). Both inlet and outlet consist of a longer “high” main channel, and a short low channel across barriers which keep the gel particles in the chamber. When a constant pressure drop is applied between inlet and outlet, the resulting flowrate will depend on the opening between the layer of particles and the cover plate, which depends on the current size of the hydrogel particles in the chamber. The fabrication, operation and experimental characterization of the microvalve is explained in detail in Richter et al. (2003), Richter et al. (2004a) and Richter et al. (2004b). All relevant parameters of the microvalve used in this article are shown in Table 1.

## Thermal subsystem

The schematic of the whole circuit describing the three domains involved (thermal, polymeric, fluidic) is shown in Figure 2. In the thermal subsystem the temperature is chosen as the difference coordinate and the flowrate

**Table 1** List of the parameters used and their values.

Parameter	Symbol	Value
Width of chamber	$w_{ch}$	500 $\mu\text{m}$
Length of chamber	$l_{ch}$	500 $\mu\text{m}$
Base area of chamber	$A_{ch}$	$(500 \mu\text{m})^2$
Height of chamber	$h_{ch}$	200 $\mu\text{m}$
Height of Si ground plate	$h_g$	300 $\mu\text{m}$
Height of Pyrex glass cover plate	$h_{py}$	500 $\mu\text{m}$
Filling height in shrunken state of hydrogels	$b$	140 $\mu\text{m}$
Estimated number of hydrogel particles	$N$	121
Specific heat capacity of Si ground plate	$c_{g,\text{specific}}$	$0.71 \times 10^3 \text{J}/(\text{kgK})$
Density of Si	$\rho_{Si}$	$2.33 \times 10^3 \text{kg}/\text{m}^3$
Volumetric heat capacity of Si ground plate	$c_g$	$1.64 \times 10^6 \text{J}/(\text{m}^3\text{K})$
Thermal conductivity of Si ground plate	$\lambda_g$	148W/(mK)
Thermal capacitance of Si ground plate	$C_{th,g}$	$1.23 \times 10^{-4} \text{J}/\text{K}$
Thermal resistance of Si ground plate	$R_{th,g}$	8.11K/W
Specific heat capacity of water	$c_{w,\text{specific}}$	$4.19 \times 10^3 \text{J}/(\text{kgK})$
Density of water	$\rho_{H_2O}$	$1 \times 10^3 \text{kg}/\text{m}^3$
Volumetric heat capacity of water	$c_w$	$4.19 \times 10^6 \text{J}/(\text{m}^3\text{K})$
Thermal conductivity of water	$\lambda_w$	0.6W/(mK)
Thermal capacitance of water in chamber	$C_{th,w}$	$2.10 \times 10^{-4} \text{J}/\text{K}$
Thermal resistance of water in chamber	$R_{th,w}$	1333K/W
Specific heat capacity of Pyrex cover	$c_{py,\text{specific}}$	$0.75 \times 10^3 \text{J}/(\text{kgK})$
Density of Pyrex	$\rho_{py}$	$2.23 \times 10^3 \text{kg}/\text{m}^3$
Volumetric heat capacity of Pyrex cover	$c_{py}$	$1.67 \times 10^6 \text{J}/(\text{m}^3\text{K})$
Thermal conductivity of Pyrex cover	$\lambda_{py}$	1.11W/(mK)
Thermal capacitance of Pyrex cover	$C_{th,py}$	$2.09 \times 10^{-4} \text{J}/\text{K}$
Thermal resistance of Pyrex cover	$R_{th,py}$	1802K/W
Thermal capacitance to ambient environment	$C_{th,amb}$	0.271J/K
Thermal resistance to ambient environment	$R_{th,amb}$	50K/W
Estimated ambient temperature	$\vartheta_{amb}$	26.5 °C
Start temperature of phase transition	$\vartheta_1$	32.5 °C
End temperature of phase transition	$\vartheta_2$	33.5 °C
Radius of gel particle in swollen state	$r_1$	55 $\mu\text{m}$
Radius of gel particle in shrunken state	$r_2$	41 $\mu\text{m}$
Volume of gel particle in swollen state	$V_1$	$6.97 \times 10^5 \mu\text{m}^3$
Volume of gel particle in shrunken state	$V_2$	$2.89 \times 10^5 \mu\text{m}^3$
Slope of equilibrium volume	$V'$	$-4.08 \times 10^5 \mu\text{m}^3/\text{K}$
Osmotic modulus in swollen state	$K_1$	$2.3 \times 10^4 \text{Pa}$
Osmotic modulus in shrunken state	$K_2$	$1.5 \times 10^5 \text{Pa}$
Slope of osmotic modulus	$K'$	$1.27 \times 10^5 \text{Pa}/\text{K}$
Cooperative diffusion coefficient (swollen state)	$D_{coop}$	$4 \times 10^{-11} \text{m}^2/\text{s}$
Polymer solvent friction coefficient	$f$	$5.75 \times 10^{14} \text{Ns}/\text{m}^4$
Dynamic viscosity of water	$\mu$	$0.8 \times 10^{-3} \text{Ns}/\text{m}^2$
Operating pressure difference	$p_{\Delta}$	1.5 bar
Fluidic resistance of channel	$R_{fl,\text{channel}}$	$4.29 \times 10^{14} \text{Pa}/(\text{m}^3\text{s})$

$I_{th} = dQ_{th}/dt$  of heat  $Q_{th}$  as the flow coordinate in the equivalent circuit description. The heater acts as a driving power source, while the temperatures of the ground plate, hydrogel and cover plate are considered as independent state variables. The heater and sensor are produced in thin-film technology and therefore have negligible thermal resistances and capacitances. We first consider a vertical structure of three layers with base area  $500\mu\text{m} \times 500\mu\text{m}$ . The thermal resistances of ground plate, water/hydrogel in the chamber and the Pyrex cover plate are designated by  $R_{th,g}$ ,  $R_{th,w}$  and  $R_{th,py}$ . The corresponding thermal capacitances are  $C_{th,g}$ ,  $C_{th,w}$  and  $C_{th,py}$ . The thermal resistance and capacitance of a component “comp” (ground plate, water and cover) are calculated by

$$R_{th,\text{comp}} = \frac{\vartheta_{\Delta,\text{comp}}}{I_{th,\text{comp}}} = \frac{l_{\text{comp}}}{\lambda_{\text{comp}}A_{\text{comp}}} \quad (1)$$

and

$$C_{th,\text{comp}} = c_{\text{comp}}V_{\text{comp}}, \quad (2)$$

where  $\vartheta_{\Delta,\text{comp}}$  is the temperature drop across the component, and  $I_{th,\text{comp}}$  is the heat flow through the component. The geometry of the component is given by its length  $l_{\text{comp}}$ , its cross section  $A_{\text{comp}}$  and its volume  $V_{\text{comp}}$ . The heat conductivity  $\lambda_{\text{comp}}$  and the volumetric heat capacity  $c_{\text{comp}}$  are intrinsic material parameters.

In order to incorporate the thermal coupling of the valve to the ambient environment of temperature

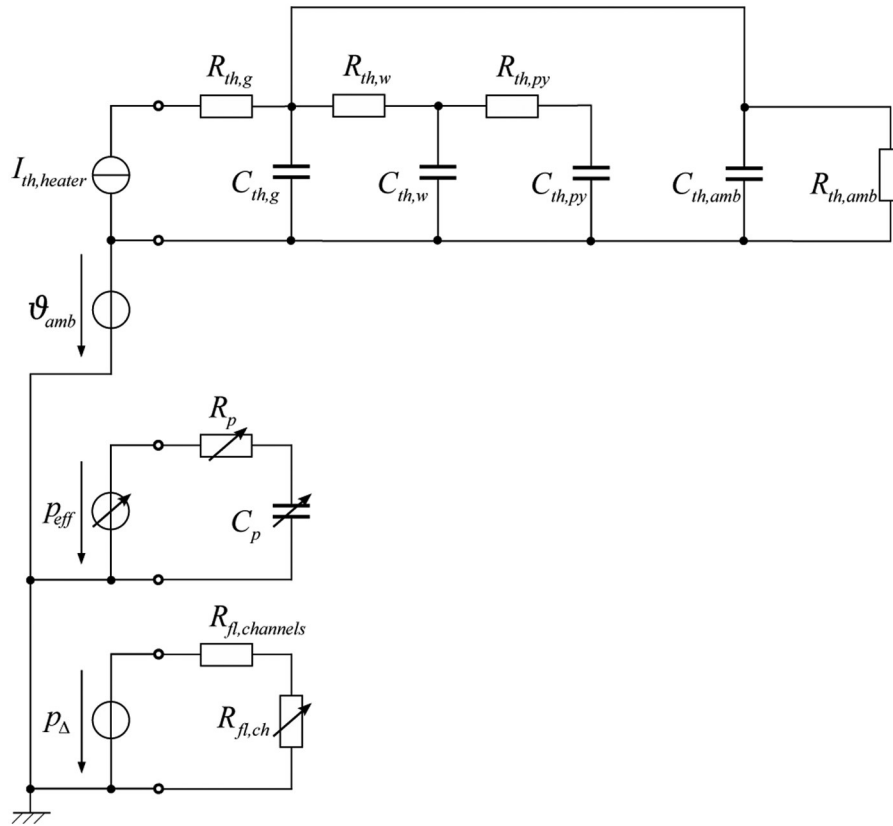


**Figure 2.** Equivalent circuit of the system. The upper part of the circuit (thermal domain) describes how the thermal source  $I_{th,heater}$  heats the various layers of the microvalve. The middle part of the circuit (polymeric domain) models the swelling/shrinking of the gel particle (compliance  $C_p$ ), obstructed by polymer-solvent friction  $R_p$ . The lower part (fluidic domain) describes how the constant pressure source effects a resulting varying flow rate, due to the current state of the valve chamber with fluidic resistance  $R_{fl,ch}$ .

$\vartheta_{amb} \approx 26.5^\circ\text{C}$  we assume that the Si layer is dominant, since its thermal conductivity is a factor of more than a hundred higher than the other layers. The value of the thermal resistance  $R_{th,amb}$  is calculated from the fact that at a heating power of 150mW the system is roughly at  $34^\circ\text{C}$  in the stationary state:

$$R_{th,amb} = \frac{34^\circ\text{C} - 26.5^\circ\text{C}}{150\text{mW}} = 50 \frac{\text{K}}{(\text{J/s})}. \quad (3)$$

The thermal capacitance  $C_{th,amb}$  to the ambient environment is estimated from the knowledge that the system initially heats up at a rate of about 1.4K/s when driven by a heat source of 380mW:

$$C_{th,amb} = \frac{0.38\text{J/s}}{1.4\text{K/s}} = 0.271\text{J/K}. \quad (4)$$

The input function of the thermal system is a time-variant power of the heater. The relevant responses are the temperature of the hydrogel (which initiates swelling and shrinking in the polymeric domain) and the temperature of the sensor (which is used for experimental readout).

## Polymeric subsystem

Here we show how the change of temperature of the hydrogel particles is translated into a change of the filling height in the chamber. We first consider the behavior of a single gel particle. The swelling and shrinking of temperature-responsive hydrogels is caused by three processes. The elasticity of the polymer network causes retaining forces. The tendency of polymer chains to mix with the surrounding liquid has an expansive effect. In the case of PNIPAAm the interaction of the polymer molecules with the solvent molecules has a retaining effect whose strength is strongly influenced by temperature. The thermodynamic free energy  $E$  depends on these three effects and is a function of the volume  $V_{hg}$  and temperature  $\vartheta_{hg}$  of the particle. The equilibrium volume of the particle for a given temperature is at the minimum of the free energy. In this work we approximate the free energy by a parabolic function of  $V_{hg}$

$$E = E_0 - p_{eff}V_{hg} + \frac{1}{2} \frac{V_{hg}^2}{C_p}, \quad (5)$$

where  $p_{eff}$  is a temperature-dependent positive effective pressure and  $C_p$  is the temperature-dependent

polymeric compliance. The minimum of the free energy is located at

$$V_{\text{eq}} = p_{\text{eff}} C_p. \quad (6)$$

Gel swelling and shrinking is always accompanied by water leaving or entering the gel. Therefore the expression *osmotic modulus* is usually preferred in lieu of the term *bulk modulus*, which is common in the theory of elasticity (Doi, 2009). The osmotic modulus amounts to

$$K = V_{\text{eq}} \left( \frac{\partial^2 E}{\partial V_{\text{hg}}^2} \right) = \frac{V_{\text{eq}}}{C_p} = p_{\text{eff}}. \quad (7)$$

From this derivation we also get

$$C_p = \frac{V_{\text{eq}}}{K}. \quad (8)$$

If the particles start out in an equilibrium state and the temperature of the gel is changed,  $K$  and  $C_p$  change and the particle will be in a non-equilibrium state with  $V_{\text{eq}}$  shifted to a different value. The particle volume will then gradually, obstructed by polymer-solvent friction, relax to its new equilibrium value, see Figure 3.

To describe the time-dependence of the relaxation process, we consider a spherical particle and assume that all processes take place with spherical symmetry. The equilibrium radius of the sphere is denoted by  $r_{\text{eq}}$ . The process is characterized by the radial displacement function  $u(r, t)$  which represents the amount by which every point of the polymer network at radius  $r$  in the reference frame (ranging from 0 to  $r_{\text{eq}}$ ) is displaced radially from its equilibrium position. The parameters of the process are the modulus  $K$  and the polymer solvent friction coefficient  $f$ . According to the model by

Tanaka and Fillmore (1979), which is based on the theory of elasticity, the relaxation process of the particle from a non-equilibrium state to equilibrium is described by the following differential equation:

$$\frac{\partial u}{\partial t} = \hat{B}u, \quad (9)$$

where the differential operator  $\hat{B}$  is defined by

$$\hat{B}u = \frac{K}{f} \frac{\partial}{\partial r} \left\{ \frac{1}{r^2} \left[ \frac{\partial}{\partial r} (r^2 u) \right] \right\}. \quad (10)$$

The boundary conditions are

$$u = 0 \quad (\text{at } r = 0) \quad (11)$$

and

$$\frac{\partial(r^2 u)}{\partial r} = 0 \quad (\text{at } r = r_{\text{eq}}). \quad (12)$$

The operator  $\hat{B}$  has an orthonormal basis of eigenfunctions

$$f_n(r) = \sqrt{\frac{\pi}{2a^3}} n (-1)^n \left( \frac{\cos(k_n r)}{k_n r} - \frac{\sin(k_n r)}{(k_n r)^2} \right) \quad (13)$$

with

$$k_n = \frac{n\pi}{r_{\text{eq}}}. \quad (14)$$

The basis functions carry the (normalized) elastic energy

$$\epsilon_n = \frac{1}{2} K \int_0^{r_{\text{eq}}} \left( \frac{1}{r^2} \frac{\partial(r^2 f_n(r))}{\partial r} \right)^2 4\pi r^2 dr = \frac{\pi^2}{2} \frac{K}{r_{\text{eq}}^2} n^2. \quad (15)$$

Any solution to equation (9) can be written in the form

$$u(r, t) = \sum_{n=1}^{\infty} G_n f_n(r) \exp(-t/\tau_n) \quad (16)$$

with the relaxation time constants

$$\tau_n = \frac{r_{\text{eq}}^2}{\pi^2 (K/f)} \frac{1}{n^2} = \frac{f}{2\epsilon_n}, \quad (17)$$

where the  $G_n$  are the initial amplitudes of the modes, determined by the initial conditions. In a circuit description these relaxation processes could be technically modeled by an infinite number of RC branches in parallel with different values of the capacitance in each branch. The charge on each capacitor would correspond to the instantaneous amplitude of the corresponding mode. However, here we aim to find a lumped model with only a single resistor and capacitor in series (see Figure 2). In the following we describe the choice of the values of the resistance and capacitance.

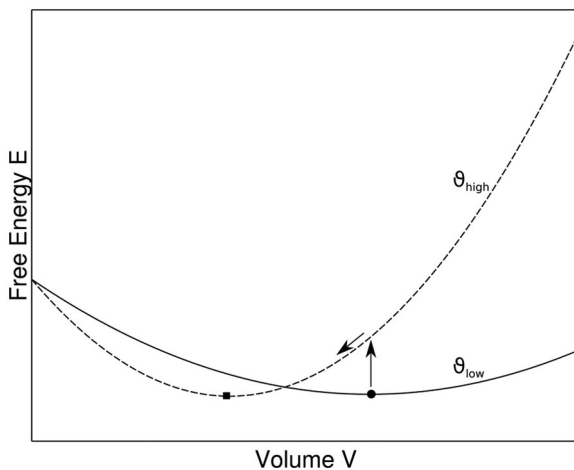


**Figure 3.** Free energy in parabolic approximation. A change of temperature leads to a different shape of the parabola (dashed line). A hydrogel in equilibrium (circle) will be in a non-equilibrium state directly after changing the temperature. Then it will gradually relax to its new equilibrium volume (square).

Our basic simplification is, that the sphere always has homogeneous strain

$$u(r, t) = G(t)r/r_{\text{eq}}, \quad (18)$$

where  $G(t)$  is the time dependent magnitude.

In the analogy of an electric capacitor that is loaded via a resistance, the volume  $V_{\text{hg}}$  corresponds to the electric charge  $Q$  on the capacitor and the flowrate  $\dot{V}_{\text{hg}}$  corresponds to the electric current  $I$ . The polymeric resistance can be calculated from the power  $P$  dissipated by the system:

$$R_p = \frac{P}{\dot{V}_{\text{hg}}^2}. \quad (19)$$

The power  $P$  can be calculated from the local friction during the expansion or contraction of the gel network

$$P = \int_{\text{sphere}} \mathbf{F} \mathbf{v} dV = f \int_0^{r_{\text{eq}}} \dot{u}^2 4\pi r^2 dr, \quad (20)$$

where  $\mathbf{F}$  is the force density and  $\mathbf{v}$  is the local velocity of the gel network. The dot denotes the derivative by time. The flow rate of the liquid into the gel follows from the movement of the outer shell of the gel

$$\dot{V}_{\text{hg}} \approx 4\pi r_{\text{eq}}^2 \dot{u}(r_{\text{eq}}). \quad (21)$$

This yields a resistance of

$$R_p = f \frac{1}{20\pi} \frac{1}{r_{\text{eq}}} = f \frac{1}{20\pi} \left( \frac{3}{4\pi} \right)^{1/3} \frac{1}{V_{\text{eq}}^{1/3}}. \quad (22)$$

This results in a time constant of

$$\tau = RC = \frac{1}{15} \frac{r_{\text{eq}}^2}{K/f}. \quad (23)$$

Note that, in an analogy to equation (17), this  $\tau$  corresponds to the normalized elastic energy of a homogeneously expanded sphere

$$\tau = \frac{f}{2\epsilon_{\text{hom}}} \quad (24)$$

with

$$\epsilon_{\text{hom}} = \frac{1}{2} K \int_0^{r_{\text{eq}}} \left( \frac{1}{r^2} \frac{\partial(r^2 u_{\text{hom}}(r))}{\partial r} \right)^2 4\pi r^2 dr - \int_0^{r_{\text{eq}}} u_{\text{hom}}^2(r) 4\pi r^2 dr \quad (25)$$

The phase transition of PNIPAAm gels leads to a change of osmotic modulus  $K$  and equilibrium volume  $V_{\text{eq}}$ . We assume a linear behavior in the transition range and constant values outside

$$K(\vartheta_{\text{hg}}) = K_1 \quad (\vartheta_{\text{hg}} < \vartheta_1), \quad (26)$$

$$K(\vartheta_{\text{hg}}) = K_1 + K' \cdot (\vartheta_{\text{hg}} - \vartheta_1) \quad (\vartheta_1 \leq \vartheta_{\text{hg}} \leq \vartheta_2), \quad (27)$$

$$K(\vartheta_{\text{hg}}) = K_2 = K_1 + K' \cdot (\vartheta_2 - \vartheta_1) \quad (\vartheta_{\text{hg}} > \vartheta_2), \quad (28)$$

and

$$V_{\text{eq}}(\vartheta_{\text{hg}}) = V_1 \quad (\vartheta_{\text{hg}} < \vartheta_1), \quad (29)$$

$$V_{\text{eq}}(\vartheta_{\text{hg}}) = V_1 + V' \cdot (\vartheta_{\text{hg}} - \vartheta_1) \quad (\vartheta_1 \leq \vartheta_{\text{hg}} \leq \vartheta_2), \quad (30)$$

$$V_{\text{eq}}(\vartheta_{\text{hg}}) = V_2 = V_1 + V' \cdot (\vartheta_2 - \vartheta_1) \quad (\vartheta_{\text{hg}} > \vartheta_2). \quad (31)$$

Here  $K_1$ ,  $K_2$ ,  $V_1$  and  $V_2$  are the osmotic moduli and equilibrium volumes outside the transition region, respectively. Corresponding to  $V_1$  and  $V_2$ , we have gel radii of  $r_1$  and  $r_2$ . The positive constant  $K'$  and the negative constant  $V'$  are the slopes of the elastic modulus and equilibrium volume in the transition range.  $\vartheta_1$  and  $\vartheta_2$  denote the temperatures at which the transition starts and ends. A lower crosslinker density in the gel leads to a sharper phase transition (smaller width  $\vartheta_2 - \vartheta_1$ ), lower  $K$  and higher swelling ratio  $V_2/V_1$ . We estimate the values of  $K_1$ ,  $K_2$ ,  $V_1$ ,  $V_2$ ,  $\vartheta_1$ ,  $\vartheta_2$  from the PNIPAAm gel B, described by Hirotsu (1991), where we neglect the dip of  $K$  observed before  $K$  starts to rise. The value  $f$  is estimated via  $f = K_1/D$  from the osmotic modulus in the swollen state and the cooperative diffusion coefficient  $D = 4 \cdot 10^{-11} \text{m}^2/\text{s}$  given in Gehrke (1993). The polymeric compliance amounts to

$$C_p(\vartheta_{\text{hg}}) = V_{\text{eq}}(\vartheta_{\text{hg}})/K(\vartheta_{\text{hg}}), \quad (32)$$

and the resistance

$$R(V_{\text{hg}}(\vartheta_{\text{hg}})) \quad (33)$$

from equation (22) is used. The circuit is driven by an external pressure source of  $p_{\text{eff}} = K(\vartheta_{\text{hg}})$ .

To calculate the filling height  $h_{\text{fill}}$  in the chamber from the volume of a single gel particle we consider a number  $N$  of equal gel particles with volume  $V_{\text{hg}}$  in the valve seat which has a base area of  $A_{\text{ch}}$ . Then the filling height  $h_{\text{fill}}$  can be approximated by

$$h_{\text{fill}} = \frac{NV_{\text{hg}}}{A_{\text{ch}}}. \quad (34)$$

This height determines the opening state of the valve. For the modeling of the gel behavior once the full height of the chamber is reached, there are two basic options: Either an abrupt stop of the swelling is assumed and  $h_{\text{fill}}$  is limited to the chamber height, or

further relaxation of the hydrogels and partial swelling into the side channels is assumed. Here we follow the latter approach and take  $h_{\text{fill}}$  as an internal state variable that can reach values higher than the chamber height. From a signal processing point of view, the polymeric system transforms a time-variant hydrogel temperature into a response of the filling height, which is the input for the fluidic system.

## Fluidic subsystem

The fluidic subsystem considers the pressure  $p_{\Delta}$  over an element as the difference coordinate and volume flow-rate  $q$  as the flow coordinate. We assume a constant pressure drop over the valve while we want to regulate the flowrate via a change of the valve state (see Figure 2). The volume flow through the valve is hindered by its fluidic friction. The valve resistance is due to the resistance of both the chamber and the connecting channels. Assuming laminar flow in an incompressible Newtonian fluid, the flowrate through a fluidic component can be calculated from the pressure drop and the fluidic resistance of the component via

$$q = \frac{p_{\Delta, \text{comp}}}{R_{\text{fl, comp}}}. \quad (35)$$

For a rectangular cross section the fluidic resistance can be approximated via

$$R_{\text{fl, comp}} = \frac{12\mu l_{\text{comp}}}{h_{\text{comp}}^3 w_{\text{comp}} (1 - 0.63h_{\text{comp}}/w_{\text{comp}})}, \quad (36)$$

where  $\mu$  is the dynamic viscosity of water,  $l_{\text{comp}}$  is the length of the component,  $h_{\text{comp}}$  is the height (small dimension) of the cross section and  $w_{\text{comp}}$  is the width (large dimension) of the cross section (Bruus, 2008).

The resistance of the chamber depends on the filling height and is calculated via

$$R_{\text{fl, ch}} = \frac{12\mu l_{\text{ch}}}{h_{\text{open}}^3 w_{\text{ch}} (1 - 0.63h_{\text{open}}/w_{\text{ch}})}, \quad (37)$$

with

$$h_{\text{open}} = \max(h_{\text{ch}} - h_{\text{fill}}, 0). \quad (38)$$

In the shrunken state the gel particles fill the chamber up to a height of  $b = 140\mu\text{m}$ . The channels and connections leading to the chamber are frictive elements that act as a series fluidic resistance. As it is difficult to estimate the value of this series resistance by purely geometric means, we determine it by fitting the theoretical flow rate through the valve in the open state to experimental data. This yields a fluidic resistance of the channels of  $4.29 \times 10^{14} \text{Pa}/(\text{m}^3\text{s})$ .

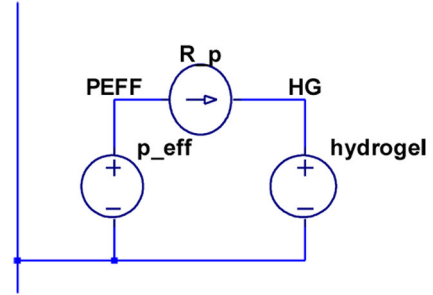


Figure 4. Implementation of the polymeric domain

The fluidic system has the filling height as the input function and the flow rate through the valve as the output function. In total, the successive combination of the three systems has four independent internal state variables ( $\vartheta_g$ ,  $\vartheta_{\text{hg}}$ ,  $\vartheta_{\text{py}}$  and  $V_{\text{hg}}$ ) and shows how the time-variant power of the heater is transformed into a time-variant flow rate.

## Implementation

For the simulation of the dynamic behavior of the system the circuit simulation software LTspice was used. The thermal system could be implemented exactly as shown in the schematic (Figure 2).

For the polymeric system (Figure 4) controlled sources were used to implement the pressure source, the variable resistor and the variable capacitance. The effective pressure source was implemented by an arbitrary behavioral voltage source using

$$p_{\text{eff}} = \min(\max(K_1 + K' \cdot (\vartheta_{\text{hg}} - \vartheta_1), K_1), K_2). \quad (39)$$

The size-dependent polymeric resistance  $R_p$  was implemented by an arbitrary behavioral current source using

$$\dot{V}_{R_p} = \frac{p_{\Delta, R_p}}{R_p(V_{\text{eq}}(\vartheta_{\text{hg}}))}, \quad (40)$$

where  $\dot{V}_{R_p}$  is the flow through the resistor, which is equal to the flow into each hydrogel particle,  $p_{\Delta, R_p}$  is the osmotic pressure drop due to friction and  $R_p(V_{\text{eq}}(\vartheta_{\text{hg}}))$  is calculated according to equation (22). The variable capacitor is implemented as an arbitrary behavioral voltage source which integrates over the current flow into the hydrogel

$$p_{\Delta, \text{hg}} = \frac{\int_0^t \dot{V}_{R_p}(t') dt'}{C_p(\vartheta_{\text{hg}}(t))}. \quad (41)$$

This guarantees that charge that is accumulated on the variable capacitor is correctly accounted for when the value of the capacitance is switched.

In the fluidic system the pressure source is implemented as a constant voltage source (see Figure 5). The



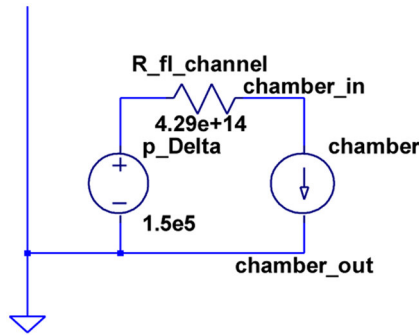


**Figure 5.** Implementation of the fluidic domain.

variable fluidic resistance of the chamber is implemented by an arbitrary behavioral current source using

$$q = \frac{P_{\Delta, ch}}{R_{fl, ch}(h_{open}(t))}. \quad (42)$$

In addition, auxiliary layers between the thermal domain and the polymeric domain, and between the polymeric domain and the fluidic domain were introduced. These are not shown here, as they have no influence on the device behavior and are solely used for the readout of the intermediate values  $V_{eq}$ ,  $K$ ,  $C_p$ ,  $V_{hg}$ ,  $r_{hg}$  and  $h_{open}$ .

## Results and discussion

The circuit based model allows the calculation of all quantities (state variables) involved for a given input function of the heating power. It is noteworthy that quantities can be monitored in the simulation that are difficult or impossible to measure during the experiment, such as the size of the hydrogel particles or the flow of liquid into the hydrogel particles. The particle size is difficult to measure in situ for a number of reasons: First, though the Pyrex cover is transparent, the temperature sensor obstructs optical access. Second, the particles move during swelling and partially cover each other. Third, the particles and their boundaries become transparent during the swelling process.

Figure 6 shows the simulated and measured response of the system to the input of the time-variant heating power. In the simulation, the heater was driven with a signal of period 60s (380mW for 8s, 150mW for 22s, 0mW for 30s (see Figure 6(a)). Note, that in Richter et al. (2003) the phase of high power heating is mentioned to be 500ms. However, the experimental curve of the temperature sensor suggests a much longer heating time, such as taken for the simulation. This is an indication of secondary effects, for example, in the control of the heater, not included in the model. The temperature of the sensor reacts with the typical retardation known from RC low pass or first order lag elements (Figure 6(b)). Once a threshold is crossed, the

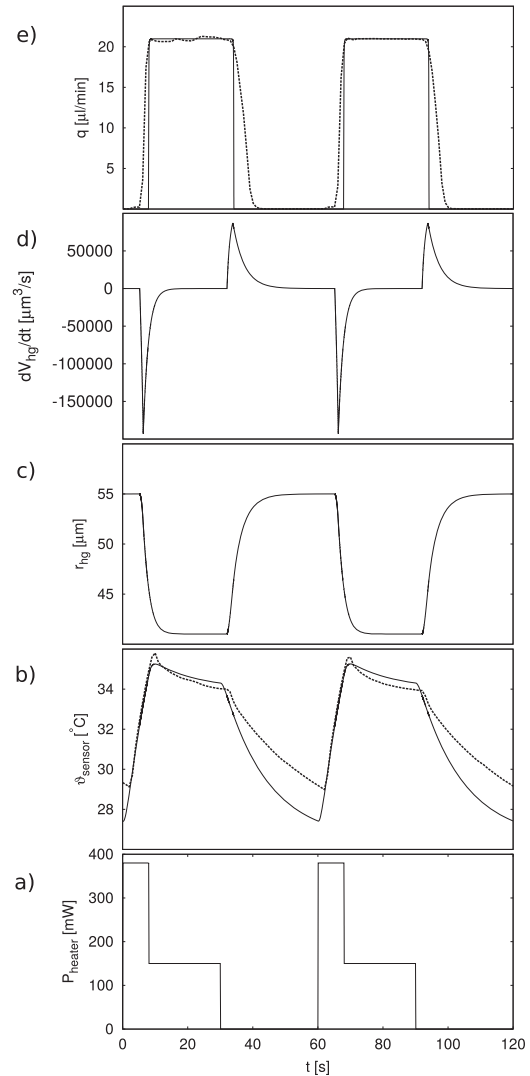


**Figure 6.** Simulated and measured time-signals. Thin solid lines: simulation. Thick dashed lines: measurement.  $P_{heater}$ : heating power.  $\vartheta_{sensor}$ : sensor temperature.  $r_{hg}$ : radius of hydrogel particle.  $dV_{hg}/dt$ : flow rate of liquid into a hydrogel particle.  $q$ : flowrate through the valve.

temperature change of the hydrogel leads to gel swelling or shrinking which is itself delayed due to the RC-type polymeric circuit (Figure 6(c)). A size change of the gel is accompanied by a corresponding flow of liquid into or out of the gel (Figure 6(d)). The size of the hydrogel particles determines the opening state of the chamber and therefore the flowrate through the valve (Figure 6(e)). The control mechanism can be divided into two phases: (a) the time the thermal system needs to react to a changed heating power such that the temperature reaches the phase transition regime, and (b) the reaction phase of the hydrogel itself. As can be seen from the plots, the first mechanism is dominant.

The simulated sensor temperature curve shows that the experimental behavior could be captured quite well with a few lumped components. The remaining

disagreement is most likely due to the fact that the system is in reality a distributed infinite-dimensional system, and that heat conduction to the ambient environment from other layers was neglected, and to the assumption of an idealized heater source.

The simulated valve flow rates are in good agreement with the experimental data. The larger width of the measured curves is probably due to the fact that for the gel characteristics values from Hirotsu (1991) were used (crosslinker density 2mol), since the gel used for the experimental setup (crosslinker density 4mol) was not characterized. If the gel used in the experiment had a slightly lower phase transition temperature, this could explain the earlier opening and later closing of the valve compared to simulation. A potential offset in the calibration of the temperature sensor would have a similar effect. As an addendum it should be mentioned that several of the used system parameters are estimations and therefore entail an amount of uncertainty with regards to experimental accuracy.

## Conclusion

An equivalent circuit model of a temperature-controlled fluidic hydrogel microvalve was developed and simulation results for a setup close to an experimental setup are presented. The resulting network model includes three physical subsystems: the thermal subsystem, the polymeric subsystem and the fluidic subsystem. All subsystems are described and coupled within one single circuit. Thus the transient behavior of the valve could be calculated using a circuit simulator. The input quantity is the time-dependent power of the heater; the response is the flowrate through the valve. The response behavior is mainly determined by two mechanisms: firstly, by the RC-type response of the thermal capacitances and the hydrogel particles which act like liquid storages, and secondly, by threshold activation processes, both of the stimulation of the hydrogel phase transition and of the opening of the valve. In addition to allowing the prediction of the system response to arbitrary input power functions, the model provides access to internal quantities (such as the current particle size) that are difficult to measure experimentally. The experimental curves of the system response (the flow rate through the valve) showed a deviation of about 20% in time scale to the simulated curves.

## Outlook

To improve the model, two types of amelioration could be implemented: The thermal circuit could be enhanced with more capacitor-resistor elements to provide a closer approximation to the distributed infinite-dimensional system it represents and to account for the coupling to the ambient environment of all layers. The

polymeric system could be expanded by changing from the parabolic approximation to a thermodynamics-based representation of the free energy function.

Network modeling can be combined with FEM modeling to reach synergetic effects by incorporating the strengths of each approach (Starke et al. 2011); for example, FEM models can be used to validate the approximations made in the network model, or to extract needed parameters. Mehner et al. (2015) describe the simulation of the closing behavior of a hydrogel valve using ANSYS. Future results will help to either validate or refine the approximations made in the current network model, especially for the state-reduction of the polymeric subsystem and the relatively simple model for the fluidic resistance.

The circuit description facilitates the aggregation of all components of a microvalve into a single compact model describing the whole valve. We use tools from electronic design automation for the automation in the design of microfluidic circuits (Paschew et al. 2016). The creation of a library of compact models for key components will significantly enhance the microfluidic design process and lead to a faster design and more versatile microfluidic chips.

## Acknowledgements

We thank Georgi Paschew for a helpful discussion on the modeling of the thermal circuit.

## Declaration of conflicting interests

The author(s) declared no potential conflicts of interest with respect to the research, authorship, and/or publication of this article.

## Funding

The author(s) disclosed receipt of the following financial support for the research, authorship, and/or publication of this article: This work is supported in part by the German Research Foundation (DFG, EXC 1056) within the Cluster of Excellence “Center for Advancing Electronics Dresden” (cfaed, EXC 1056). Additional funding was provided by the European Social Fund within the project 100108861 “Organomechanics”.

## References

- Arndt KF, Kuckling D and Richter A (2000) Application of sensitive hydrogels in flow control. *Polymers for Advanced Technologies* 11(8–12): 496–505.
- Baldi A, Gu Y, Loftness P, et al. (2003) A hydrogel-actuated environmentally sensitive microvalve for active flow control. *Journal of Microelectromechanical Systems* 12(5): 613–621.
- Beebe DJ, Moore JS, Bauer JM, et al. (2000) Functional hydrogel structures for autonomous flow control inside microfluidic channels. *Nature* 404(6778): 588–590.
- Brocard G and Engelhardt M (2011) *Le Simulateur LTspice IV Manuel, Méthodes et Applications*. Paris: Dunod.

- Bruus H (2008) *Theoretical Microfluidics*. Oxford: Oxford University Press.
- Doi M (2009) Gel dynamics. *Journal of the Physical Society of Japan* 78(5): 052001.
- Ehrenhofer A, Bingel G, Paschew G, et al. (2016) Permeation control in hydrogel-layered patterned PET membranes with defined switchable pore-geometry - Experiments and numerical simulation. *Sensors and Actuators B* 232: 499–505.
- Gehrke SH (1993) Synthesis, equilibrium swelling, kinetics, permeability and applications of environmentally responsive gels. In: PK Dušek (ed.) *Responsive Gels: Volume Transitions II (Advances in Polymer Science, vol. 110)*. Berlin, Heidelberg, Germany: Springer, pp.81–144.
- Hirotsu S (1991) Softening of bulk modulus and negative Poisson's ratio near the volume phase transition of polymer gels. *The Journal of Chemical Physics* 94(5): 3949–3957.
- Hodgkin AL and Huxley AF (1952) A quantitative description of membrane current and its application to conduction and excitation in nerve. *The Journal of Physiology* 117(4): 500–544.
- Lenk A, Ballas RG, Werthschützky R, Pfeifer G, et al. (2011) *Electromechanical Systems in Microtechnology and Mechatronics*, Microtechnology and MEMS. Berlin, Heidelberg: Springer.
- Li SS and Cheng CM (2013) Analogy among microfluidics, micromechanics, and microelectronics. *Lab on a Chip* 13(19): 3782–3788.
- Marschner U, Grätz H, Jettkant B and et al. (2009) Integration of a wireless lock-in measurement of hip prosthesis vibrations for loosening detection. *Sensors and Actuators A: Physical* 156(1): 145–154.
- Marschner U, Starke E and Pfeifer G (2013) Efficient Dynamic Modeling and Simulation of Smart Structures with (Equivalent) Circuits. In: *ASME 2013 conference on smart materials, adaptive structures and intelligent systems, volume 1*, Snowbird, UT, 16–18 September, 2013, paper no. SMASIS2013-3260.
- Mehner PJ, Allerdißen M, Voigt A, et al. (2015) Combined simulation of the closing behavior of a smart hydrogel micro-valve. In: *ASME 2015 conference on smart materials, adaptive structures and intelligent systems, volume 1*, Colorado Springs, CO, 21–23 September, 2015, paper no. SMASIS2015-8991. ASME.
- Oh KW, Lee K, Ahn B, et al. (2012) Design of pressure-driven microfluidic networks using electric circuit analogy. *Lab on a Chip* 12(3): 515–545.
- Paschew G, Schreiter J, Voigt A, et al. (2016) Autonomous chemical oscillator circuit based on bidirectional chemical-microfluidic coupling. *Advanced Materials Technologies* 1(1): 1600005
- Perdigones F, Luque A and Quero J (2014) Correspondence between electronics and fluids in MEMS: Designing microfluidic systems using electronics. *IEEE Industrial Electronics Magazine* 8(4): 6–17.
- Pierret R and Sah C (1970a) Quantitative analysis of the effects of steady-state illumination on the MOS-capacitor—I. *Solid-State Electronics* 13(3): 269–288.
- Pierret R and Sah C (1970b) Quantitative analysis of the effects of steady-state illumination on the MOS-capacitor—II. *Solid-State Electronics* 13(3): 289–302.
- Richter A, Howitz S, Kuckling D, et al. (2004a) Influence of volume phase transition phenomena on the behavior of hydrogel-based valves. *Sensors and Actuators B: Chemical* 99(2–3): 451–458.
- Richter A, Howitz S, Kuckling D, et al. (2004b) Automatically and electronically controllable hydrogel based valves and microvalves—Design and operating performance. *Macromolecular Symposia* 210(1): 447–456.
- Richter A, Kuckling D, Howitz S, et al. (2003) Electronically controllable microvalves based on smart hydrogels: Magnitudes and potential applications. *Journal of Microelectromechanical Systems* 12(5): 748–753.
- Sah C (1970) The equivalent circuit model in solid-state electronics—III. *Solid-State Electronics* 13(12): 1547–1575.
- Starke E, Marschner U and Pfeifer G (2011) Combining network models and FE-models for the simulation of electromechanical systems. In: *Proc. SPIE 7977, active and passive smart structures and integrated systems 2011* (ed MN Ghasemi-Nejhad), San Diego, CA, 6 March 2011, pp.79771Y–79771Y–8. International Society for Optics and Photonics.
- Tanaka T and Fillmore DJ (1979) Kinetics of swelling of gels. *The Journal of Chemical Physics* 70(3): 1214–1218.